

Sign-Indefinite Helicity and the Structure of Weak Turbulence in Inertial and Non-Hermitian Waves

Shahaf Aharony Shapira[†] and Michal Shavit^{*}

[†] *Department of Physics of Complex Systems, Weizmann Institute of Science, Rehovot 7610001, Israel*

^{*} *Courant Institute of Mathematical Sciences, New York University, NY 10012, USA.*

We investigate how sign-indefinite quadratic invariants shape turbulent cascades in incompressible flows with broken time-reversal symmetry, where the dynamics supports strongly anisotropic dispersive waves. Focusing on rotating Euler flow and odd-viscous Euler flow, we isolate the wave component and study the corresponding weak-turbulence kinetic equation. We show that helicity conservation substantially simplifies the kinetic equation. Fixing the energy flux by a natural gauge choice, we identify the turbulent spectrum as the unique scale-invariant solution that sustains a constant flux of energy from large to small scales. Under a mild approximation motivated by the accumulation of energy near slow modes, we compute the leading angular dependence and uncover an integrable singularity along the slow-mode curve, that agrees with previous results. We then demonstrate that helicity reorganizes cascade directions at the level of resonant triads. Although helicity is globally sign-indefinite, the helical decomposition splits it into sign-definite contributions on each polarization branch. Triads whose three legs lie on the same branch behave as if constrained by a sign-definite invariant and drive an upscale transfer of energy, producing systematic backscatter even when the net cascade is direct. In the helicity-definite limit (single-branch dynamics), the kinetic equation admits an additional scale-invariant solution associated with helicity transport. Finally, we validate the analytical predictions by numerically evaluating the collision integral in the strongly anisotropic limit, revealing a family of stationary solutions in that regime.

Introduction A central question in turbulence is how conservation laws constrain the direction of energy transfer across scales. Understanding how quadratic invariants shape turbulent cascades has been a central theme of fluid dynamics since the pioneering works of Kolmogorov and Kraichnan [1, 2]. In isotropic three-dimensional (3D) turbulence, energy cascades directly toward small scales, while helicity, being sign-indefinite, does not by itself enforce an inverse cascade. By contrast, in systems where the second quadratic invariant is sign-definite—such as enstrophy in two-dimensional turbulence—energy transfer is strongly constrained and an inverse cascade emerges: Fjørtoft’s classical argument shows that the simultaneous conservation of energy and enstrophy forces energy to migrate to larger scales, while enstrophy flows to smaller ones [3]. More broadly, in weakly nonlinear wave systems the same principle leads to inverse cascades associated with conserved invariants, captured by the Kolmogorov–Zakharov spectra of wave turbulence theory [4]. These examples suggest that even invariants that are globally sign-indefinite may nonetheless influence cascade directions when the dynamics organizes interactions into subsets where they become effectively sign-definite.

A natural setting in which such questions arise is turbulence in systems where time-reversal symmetry is broken and the dynamics supports chiral dispersive waves. Two paradigmatic examples are rotating fluids [5–7], where the Coriolis force singles out the axis of rotation, and fluids with odd (Hall) viscosity, where parity and time-reversal symmetry are simultaneously broken by the stress tensor [8–11]. In both cases,

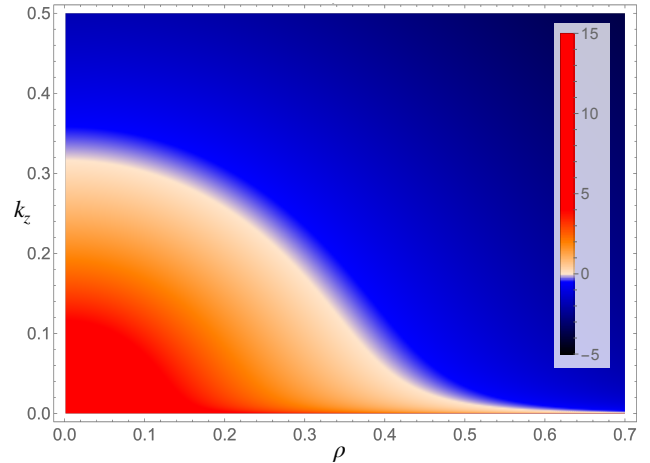


FIG. 1. Logarithm of the energy spectrum $e_k = C_0 k^{-3} |\cos \theta_k|^{-1/2}$ on the $(\rho := \sqrt{k_x^2 + k_y^2}, k_z)$ plane, outside an angular source centered at radius k_f and emitting a radial energy flux $\Pi^r(\theta_k) = \Pi_0 |\cos \theta_k|^{-1} \hat{k}/k$.

the linearized dynamics support dispersive waves that propagate anisotropically: inertial waves in rotating flows and “odd waves” in odd-viscous fluids. The presence of such waves naturally leads to a weak-turbulence regime governed by (pseudo-)resonant wave interactions, which we can study analytically.

These systems therefore provide a controlled framework for investigating how helicity influences turbulent cascades in anisotropic, wave-dominated flows. In the helical basis, helicity decomposes into sign-definite contributions associated with the two circular

polarizations of each Fourier mode. This decomposition allows one to isolate subsets of resonant interactions in which helicity becomes effectively positive-definite. As we show below, interactions within such subsets reverse the direction of energy transfer: sign-definite helicity interactions drive an inverse cascade, even though the full system admits a direct cascade. This complements earlier observations that small-scale intermittency is reduced in systems with such constraints compared to fully isotropic 3D turbulence [12].

To characterize these cascades, we introduce a natural gauge fixing for the energy flux that separates isotropic and anisotropic contributions. This allows us to identify the unique scale-invariant solutions that support a nonzero radial flux. Exploiting the scale invariance of the governing equations, and without imposing the strongly anisotropic limit, we derive the scale-invariant component of the energy spectrum. Our analysis shows that anisotropic wave turbulence fundamentally organizes energy transfer through angular structure on the unit sphere, where forcing may be applied without loss of generality. From this angular distribution, the cascade proceeds radially—though anisotropically—in a scale-invariant manner. This viewpoint improves upon previous treatments that impose strong anisotropy at the outset and consequently produce nonphysical divergences in the predicted energy spectrum.

To determine the angular structure of the spectrum, we treat anisotropy in a weaker sense and compute the asymptotic angular dependence. This reveals weak but integrable singularities near the slow-mode manifold, where wave energy is expected to accumulate, see Figure 1. We then numerically evaluate the collision integral in the standard strongly anisotropic limit to confirm and illustrate these analytical predictions.

Odd-wave turbulence connects fundamental fluid mechanics with broader themes across physics. Odd viscosity emerges as an effective transport coefficient in active matter and certain quantum fluids, while rotating flows are ubiquitous in geophysical and astrophysical contexts. Both systems illustrate how the breaking of discrete symmetries—parity and time reversal—can qualitatively reorganize cascade phenomenology. In this work we focus on the wave component of the flow. While our results indicate a concentration of wave energy near slow modes, we do not analyze the slow modes themselves. Their dynamics, particularly in the presence of condensates, have recently been investigated in the context of rotating turbulence [13, 14].

Governing equations Consider the Euler equation in 3D space written in vorticity form

$$\partial_t \boldsymbol{\omega} = (\boldsymbol{\omega} \cdot \nabla) \mathbf{v} - (\mathbf{v} \cdot \nabla) \boldsymbol{\omega}, \quad (1)$$

where \mathbf{v} is the velocity field, $\boldsymbol{\omega} = \nabla \times \mathbf{v}$ is the vorticity and incompressibility is assumed, $\nabla \cdot \mathbf{v} = 0$. The

Euler equation has two quadratic invariants: the positive-definite kinetic energy, $E = \frac{1}{2} \int |\mathbf{v}|^2 d\mathbf{x}$, and the (sign-indefinite) helicity, $H = \int \mathbf{v} \cdot \boldsymbol{\omega} d\mathbf{x}$. Eq. (1) can be written as a noncanonical Hamiltonian system on the dual of the divergence-free vector fields [15]:

$$\partial_t \boldsymbol{\omega} = \mathcal{J} \left(\frac{\delta E}{\delta \boldsymbol{\omega}} \right), \quad (2)$$

where the Poisson operator \mathcal{J} is the skew-symmetric form

$$\mathcal{J}(\mathbf{a}) = -\nabla \times (\boldsymbol{\omega} \times (\nabla \times \mathbf{a})). \quad (3)$$

From (2) it follows that the kinetic energy is conserved due to time-translation invariance. The helicity, which is a *Casimir* of the Poisson structure (3), is also conserved because the velocity lies in the kernel of \mathcal{J} . See [16] for more details. Geometrically, this reflects the Lie advection of vorticity by the flow, which preserves the topology of vortex lines and hence helicity.

Helical decomposition. In a periodic box of size L^3 , we expand the velocity in eigenfunctions of the curl operator \mathbf{h}_{s_α} ,

$$\mathbf{v}(\mathbf{x}, t) = \sum_{\alpha} v_{\alpha}(t) \mathbf{h}_{s_{\alpha}}(\mathbf{k}_{\alpha}) e^{i\mathbf{k}_{\alpha} \cdot \mathbf{x}}, \quad (4)$$

where $\alpha = (s_{\alpha}, \mathbf{k}_{\alpha})$ is a multi-index carrying the chirality $s = \pm 1$ and the wave number $\mathbf{k} \in \mathbb{Z}^3/L$. Accordingly, $v_{\alpha}(t)$ is the projection of $\mathbf{v}(\mathbf{k}_{\alpha}, t)$ on $\mathbf{h}_{s_{\alpha}}$. The Euler equation becomes [17]

$$\partial_t v_{\alpha} = \sum_{\beta, \gamma} C_{\alpha}^{\beta\gamma} v_{\beta}^* v_{\gamma}^*, \quad (5)$$

where $C_{\alpha}^{\beta\gamma} = -\frac{1}{4}(s_{\beta}k_{\beta} - s_{\gamma}k_{\gamma}) g_{\alpha\beta\gamma}$, with $g_{\alpha\beta\gamma} = \mathbf{h}_{s_{\alpha}}^*(\mathbf{k}_{\alpha}) \cdot (\mathbf{h}_{s_{\beta}}^*(\mathbf{k}_{\beta}) \times \mathbf{h}_{s_{\gamma}}^*(\mathbf{k}_{\gamma}))$ nonzero only if $\mathbf{k}_{\alpha} + \mathbf{k}_{\beta} + \mathbf{k}_{\gamma} = \mathbf{0}$. In this formulation the dynamics is organized into triadic interactions whose strength depends explicitly on the helicities of the participating modes, so that different polarization combinations produce qualitatively different nonlinear transfers. In this representation the quadratic invariants are diagonal:

$$E = \frac{1}{2} \sum_{\alpha} E_{\alpha} := \frac{1}{2} \sum_{\alpha} v_{\alpha} v_{\alpha}^*, \quad H = \sum_{\alpha} S_{\alpha} E_{\alpha}, \quad (6)$$

where $S_{\alpha} := s_{\alpha} k_{\alpha}$. Their conservation imposes the following restrictions on the interaction coefficients,

$$C_{\alpha}^{\beta\gamma} + C_{\beta}^{\alpha\gamma} + C_{\gamma}^{\alpha\beta} = 0, \quad (7)$$

$$S_{\alpha} C_{\alpha}^{\beta\gamma} + S_{\beta} C_{\beta}^{\alpha\gamma} + S_{\gamma} C_{\gamma}^{\alpha\beta} = 0. \quad (8)$$

Since helicity is a casimir of the algebra induced by the Poisson form, this might impose additional constraints on the nonlinear interactions. We do not pursue this question further here.

Dispersive waves and the kinetic equation To introduce rotation- or chirality-induced dispersive wave dynamics, we add a linear dispersive operator of the form: $\nabla \times iL(\frac{1}{\tau}\nabla \times)\mathbf{v}$ to the right-hand side of the Euler equation (1). This operator manifests non-Hermitian behavior due to its antisymmetric structure. However, since the operator is diagonal in terms of the curl eigenfunctions and $\omega_\alpha := s_\alpha L(\mathbf{k})$ is real for $\mathbf{k} \in \mathbb{R}^3$, the conservation of energy and helicity persists. This is the case, for example, for a uniformly rotating fluid with

$$iL = -2\boldsymbol{\Omega} \times \mathbf{v}, \quad (9)$$

where the rotation axis is taken as $\boldsymbol{\Omega} = \Omega \hat{z}$. The dispersion relation is then

$$\omega_\alpha^\Omega = \pm \Omega k_z / k. \quad (10)$$

Another example arises in fluids with odd viscosity,

$$iL = \boldsymbol{\nu}^{\text{odd}} \times \Delta \mathbf{v}, \quad (11)$$

which can be viewed as a differential form of rotation [9]. In the simple case $\boldsymbol{\nu}^{\text{odd}} = \nu^{\text{odd}} \hat{z}$, and

$$\omega_\alpha = \omega_{(s,\mathbf{k})} = s_\alpha \nu^{\text{odd}} k_z k. \quad (12)$$

The dispersive operator generates plane waves, which are solutions of the linear part of the Euler equation: $v_\alpha(t) = v_\alpha(t=0)e^{i\omega_\alpha t}$, where $v_\alpha(t=0)$ is the initial condition. Filtering the linear motion $v_\alpha \rightarrow e^{-i\omega_\alpha t} v_\alpha$, the Euler equation becomes

$$\partial_t v_\alpha = \sum_{\beta,\gamma} C_\alpha^{\beta\gamma} v_\beta^* v_\gamma^* e^{i(\omega_\alpha + \omega_\beta + \omega_\gamma)t}. \quad (13)$$

The oscillatory phase multiplying the nonlinear interaction introduces a separation of time scales in the evolution of the nonlinear solution for *small initial data*. This separation allows one to derive a kinetic equation describing the slow evolution of the averaged wave component of the energy density $e_\alpha = \overline{E_\alpha}$. The overbar denotes averaging over an initial Gaussian statistical ensemble,

$$\overline{v_\alpha^*(0)v_\beta(0)} = \delta_{\alpha\beta} e_\alpha(0), \quad (14)$$

and its evolution is governed by the kinetic equation

$$\begin{aligned} \dot{e}_\alpha &= St_\alpha(e_\alpha) \\ &= \sum_{\beta,\gamma} \int_{\omega_{\alpha\beta\gamma}} C_\alpha^{\beta\gamma} \left(C_\alpha^{\beta\gamma} e_\beta e_\gamma + C_\beta^{\alpha\gamma} e_\alpha e_\gamma + C_\gamma^{\alpha\beta} e_\alpha e_\gamma \right), \end{aligned} \quad (15)$$

that was derived by [11]. To derive the kinetic equation, which provides the first nontrivial closure for the evolution of the wave component of the energy, one takes the joint kinetic limits of large domain and long nonlinear times, $L \rightarrow \infty$ and $t\omega_\alpha \rightarrow \infty$. In this limit the

discrete sum over the lattice in Eq. (5) is replaced by an integral over the resonant manifold:

$$\int_{\omega_{\alpha\beta\gamma}} d\beta d\gamma \delta(\omega_\alpha + \omega_\beta + \omega_\gamma) \delta(\mathbf{k}_\alpha + \mathbf{k}_\beta + \mathbf{k}_\gamma), \quad (16)$$

where $\int d\alpha = \sum_{s=\pm 1} \int d\mathbf{k}_\alpha$.

Near small frequencies, the kinetic equation must be interpreted carefully. In the discrete sum on the lattice, i.e. Eq. (13), slow modes are well separated from waves with non-zero frequency. However, as $L \rightarrow \infty$, the collision integral (15) includes integration arbitrarily close to slow modes. While slow modes cannot be created by resonant interactions, as $\omega_\alpha \rightarrow 0$ the kinetic equation needs to include off-diagonal correlators apart from (14), such as $\overline{v_\alpha^2}$, which would yield a very complicated description. Such correlators oscillate with frequency $\sim 2\omega_\alpha$ and over long times can be neglected as long as the frequency is bounded away from zero $|\omega_\alpha| > \epsilon > 0$ [18]. From this perspective, anisotropic systems whose dispersion relation vanishes along a curve rather than at a point pose a particular challenge for the kinetic description.

On the resonant manifold, conservation of helicity can be used to simplify the kinetic equation as follows. Consider the vector of interaction coefficients for a triad (α, β, γ) ,

$$\left(C_\alpha^{\beta\gamma}, C_\beta^{\alpha\gamma}, C_\gamma^{\alpha\beta} \right) \quad (17)$$

as a vector in \mathbb{R}^3 . Conservation of energy and helicity implies that this vector is orthogonal to both

$$(1, 1, 1), \quad (S_\alpha, S_\beta, S_\gamma). \quad (18)$$

Except for degenerate cases, the three vectors

$$(1, 1, 1), \quad (S_\alpha, S_\beta, S_\gamma), \quad (k_\alpha^z, k_\beta^z, k_\gamma^z) \quad (19)$$

span \mathbb{R}^3 . On the resonant manifold $(k_\alpha^z, k_\beta^z, k_\gamma^z)$ is also orthogonal to both $(1, 1, 1)$ and $(S_\alpha, S_\beta, S_\gamma)$. Therefore, the interaction coefficients must be parallel to $(k_\alpha^z, k_\beta^z, k_\gamma^z)$ and hence can be written in terms of a symmetric coupling $\Gamma_{\alpha\beta\gamma}$ as

$$\left(C_\alpha^{\beta\gamma}, C_\beta^{\alpha\gamma}, C_\gamma^{\alpha\beta} \right) = \Gamma_{\alpha\beta\gamma} (k_\alpha^z, k_\beta^z, k_\gamma^z). \quad (20)$$

This reduces the kinetic equation to the simpler form

$$\partial_t e_\alpha = \sum_{\beta,\gamma} \int_{\omega_{\alpha\beta\gamma}} k_\alpha^z \Gamma_{\alpha\beta\gamma}^2 (k_\alpha^z e_\beta e_\gamma + k_\beta^z e_\alpha e_\gamma + k_\gamma^z e_\alpha e_\beta). \quad (21)$$

Degenerate cases include for example $S_\alpha = S_\beta = S_\gamma$, in which case the interaction coefficients vanish. The

collision integral St_α , which corresponds to the right-hand side (RHS) of this equation, admits the equilibrium solution $e_\alpha = 1$. We now turn to finding solutions that carry a nonzero flux.

Boundary conditions and steady solutions of the kinetic equation. The frequency and the geometric coupling are symmetric under the dilation transformation: $\mathbf{k} \rightarrow \lambda\mathbf{k}$, for $\lambda > 0$, where the homogeneity degree x is determined by the scaling law $F(\lambda\mathbf{k}) = \lambda^x F(\mathbf{k})$. That is,

$$\omega_{(s,\lambda\mathbf{k})} = \lambda^2 \omega_{(s,\mathbf{k})}, \quad (22)$$

$$\Gamma(\lambda\mathbf{k}_\alpha, \lambda\mathbf{k}_\beta, \lambda\mathbf{k}_\gamma) = \Gamma(\mathbf{k}_\alpha, \mathbf{k}_\beta, \mathbf{k}_\gamma). \quad (23)$$

The wavenumbers themselves are homogeneous of degree one, and therefore the delta functions that define the resonant manifold are also homogeneous. Assuming the steady spectrum e_α shares this dilation symmetry leads to a separable homogeneous form $e_\alpha = C_0 k^{-w} e_\alpha^\Omega(\theta_k, \phi_k)$, where $C_0 > 0$ is the Kolmogorov constant. Because the kinetic equation has azimuthal symmetry about the vertical axis, the angular dependence reduces to a function of the polar angle only. Motivated by the fact that the dispersion relation depends on the angle only through $\omega_\alpha / (\nu_{\text{odd}} s_\alpha k^2) = \cos\theta_k$, while the interaction coefficient is isotropic, we represent the spectrum as

$$e_\alpha = C_0 k^{-w} |\cos\theta_k|^{-f_{w,\alpha}(\theta_k)}. \quad (24)$$

Substituting this homogeneous spectrum into the collision integral turns it into a homogeneous function that separates into radial and angular parts. The collision integral takes the form

$$St_\alpha \equiv k^{2w_0-2w-d} C_0^2 St_{\Omega,\alpha}(w, f_w, \theta_k), \quad (25)$$

where $d = 3$ is the dimension and $2w_0 - 2w - d$ is the total homogeneity degree of the elements entering the kinetic equation, written in this form for later use. In our case $w_0 = d = 3$. The explicit form of the angular collision integral, St_Ω , is obtained by parametrizing the resonant manifold and is presented in the supplemental material.

The separability of the collision integral suggests the existence of a one-parameter family of scale-invariant spectra parametrized by the exponent w . To select the physically relevant solution, we impose boundary conditions through the energy flux. Since the Energy is an integral of motion, the kinetic Eq. (21) can be written formally as a continuity equation

$$\dot{e}_\alpha(t) + \text{div}\Pi_\alpha(t) = 0, \quad (26)$$

where $\Pi_\alpha(t)$ is a three-dimensional flux in \mathbf{k} -space. Its divergence is related to the collision integral through

$$\text{div}\Pi_\alpha(t) = -St_\alpha(e_\alpha). \quad (27)$$

Thus, a steady solution corresponds to a divergence-free flux. Because of the gauge freedom $\Pi_\alpha + \nabla \times A_\alpha$, with a vector potential A_α , infinitely many flux fields correspond to the same steady state. However, fixing the flux fixes the solution uniquely. In stationary turbulence sustained between forcing and dissipation scales that are widely separated, a natural gauge choice is a purely radial flux, $\Pi_\alpha = \Pi_\alpha^r \hat{r}$. This choice is also consistent with the fact that there are no resonant interactions among triads with identical wavenumber magnitude, $k_\alpha = k_\beta = k_\gamma$, but different angles. With this choice, the divergence relation becomes

$$\text{div}\Pi_\alpha = k^{-d+1} \partial_k (k^{d-1} \Pi_\alpha^r) \equiv -St_\alpha(e_\alpha). \quad (28)$$

Substituting the homogeneous spectrum (24) gives

$$k^{-d+1} \partial_k (k^{d-1} \Pi_\alpha^r) = -k^{2w_0-2w-d} C_0^2 St_\Omega(w, f_w, \theta_k), \quad (29)$$

such that in a steady state, $St_\Omega(w_0, f_{w_0}, \theta_k)$ must vanish. Multiplying by k and integrating $\int_k^\infty dk'$ assuming $w < w_0$ yields the radial flux

$$k^{d-1} \Pi_\alpha^r = -\frac{k^{2(w_0-w)}}{2(w_0-w)} C_0^2 St_\Omega(w, f_w, \theta_k). \quad (30)$$

Integrating $\int_0^k dk'$ would yield the same expression for $w > w_0$. From this expression it becomes clear that the pair (w_0, f_{w_0}) corresponds to a special solution: the unique scale-invariant spectrum that gives a non-zero scale-independent radial flux with zero divergence. This fixes the isotropic scaling exponent of the turbulent spectrum to

$$e_\alpha = C_0 k^{-3} |\cos\theta_k|^{-f_{w_0,\alpha}(\theta_k)}. \quad (31)$$

As w tends to w_0 , due to the diverging denominator in Eq. (30), the radial flux is given by:

$$\Pi_\alpha^r(w_0, f_{w_0}) = \frac{C_0^2}{2k^{d-1}} \frac{d}{dw} St_{\Omega,\alpha}(w, f_{w_0}, \theta_k) |_{w=w_0}. \quad (32)$$

The derivative with respect to w in the definition of the flux is taken after the angular part $f_w = f_{w_0}$ has been fixed in the angular collision integral. Isotropic wave turbulence [19] is a particular case of Eq. (32) where $St_\Omega(w, f_{w_0}, \theta_k) = St_\Omega(w)$ is independent of the angle. In non-isotropic systems, it is natural to expect the flux Π_α^r to depend on the angle. The average over a sphere gives the constant non-zero total radial flux

$$2\pi \int_0^\pi k^{d-1} \Pi_\alpha^r(\theta) \sin\theta d\theta = \Pi_0. \quad (33)$$

The scaling obtained above arises in two distinct helicity configurations. In the first, helicity is equally distributed between left- and right-handed waves, so that the mean helicity vanishes: $e_{+,\mathbf{k}} = e_{-,\mathbf{k}}$ and $\bar{H} = 0$. In

the second, helicity is concentrated on a single branch, corresponding to a sign-definite helicity state, e.g. $e_{-, \mathbf{k}} = 0$, so that $\bar{H} > 0$. In this case the kinetic equation admits an additional scaling solution corresponding to a helicity cascade. Since the helicity density at each wavenumber scales as $ke_{(+, k)}$, the flux relation is modified accordingly

$$k^{d-1}\Pi_\alpha^{r, H} = -\frac{k^{2(w_0-w)+1}}{2(w_0-w)+1}C_0^2St_\Omega(w_H, f_{w_H}, \theta_k), \quad (34)$$

and leads to an helicity-cascade scaling exponent $w_h = 3.5$. The corresponding spectrum is

$$e_\alpha^H = C_0 k^{-3.5} |\cos \theta_k|^{-f_{w_h, \alpha}(\theta_k)}. \quad (35)$$

This spectrum is not an exact steady solution of the kinetic equation but rather an asymptotic regime that may arise near sources of chirality-definite waves. Nevertheless, it has important implications for how energy flux is distributed among different helicity triads, which we discuss next.

Helicity and flux directions. The density of helicity is proportional to the energy density through the isotropic and monotonic function k . As a consequence, the power-law exponent associated with the energy cascade is smaller than the exponent corresponding to the helicity cascade solution of the kinetic equation restricted to a single (positive) helicity branch, i.e. $w_0 < w_h$.

Suppose that the angular part of the collision integral has the same kernel for both cascades, namely $f_{w_0} = f_3 = f_{3.5} = f_{w_h}$. In this case, sign-definite helicity interactions would transfer energy toward smaller absolute wavenumbers (an inverse energy cascade), while sign-indefinite helicity interactions would transfer energy toward larger absolute wavenumbers (a direct cascade). This conclusion follows from a generalization of the flux analysis for isotropic scale-invariant solutions described in [20]. Consider the family of spectra given by Eq. (turbspec), and fix the angular dependence to be $f_w = f_{w_0}$, while allowing the homogeneous scaling k^{-w} to vary. Within this restricted family, our analysis shows that only one spectrum corresponds to a steady state, namely $w = w_0 = 3$. All other spectra are non-stationary, but a flux can still be defined for them—whenever it is finite—by continuity from the expression derived earlier, (30), which we denote by $\Pi_\alpha(w)$.

In the limit $w \rightarrow \infty$, where most of the energy is concentrated at very small wavenumbers, the flux is expected to be positive. Since there are no additional steady solutions $w \neq w_0$ associated with other positive-definite invariants, the flux does not change sign near the energy-cascade solution and therefore remains positive at $w = w_0$. This corresponds to a forward (direct) energy cascade.

Now consider the kinetic equation restricted to interactions involving only positive-helicity waves. In this

case, in addition to the energy-cascade solution w_0 , the kinetic equation admits another scale-invariant solution corresponding to a helicity cascade at $w_h = 3.5$. Because this spectrum is an exact solution on the positive branch, the energy flux must vanish there, as follows directly from the flux expression derived earlier.

Since $w_h > w_0$ and there are no additional zeros of the flux, the function $\Pi_\alpha(w)$ crosses zero once—starting from positive values as $w \rightarrow \infty$ and vanishing at $w = w_h$. It therefore remains negative at $w = w_0$. This implies that, within the helicity-definite dynamics, the energy flux at the energy-cascade scaling is directed toward larger spatial scales.

In the next section we introduce an approximation motivated by the accumulation of energy near slow modes. Under this approximation we show that the same behavior arises in the full odd-wave system. Thus, although helicity is globally sign-indefinite, the interactions involving helicity-definite triads constrain the cascade dynamics. In particular, when both positive- and negative-helicity waves are present, helicity-definite interactions drive a portion of the energy flux toward large scales.

Slow modes and the angular part of the solution. While the self-similar, scale-invariant part of the solution is largely insensitive to the precise domain of validity of the kinetic equation, the angular structure of the spectrum is not. This sensitivity arises from the limit $\theta_k \rightarrow \pi/2$, which corresponds to $\omega_\alpha \rightarrow 0$. In this limit the derivation of the kinetic equation breaks down, because the separation of linear and nonlinear time scales underlying weak turbulence theory no longer holds. Since waves with vanishing frequency correspond to slow modes, and since energy is expected to accumulate near these modes, the solution should exhibit a singular behavior along the curve of zero frequency, $k_\alpha^z = 0$ or $\theta_k = \pi/2$.

We now determine f_{w_0} , the exponent of the angular part of the spectrum, and focus on solutions with a constant exponent f . Because the kinetic equation is independent of the azimuthal angles, we first integrate over them. This produces the averaged delta function

$$\int d\phi_\beta \int d\phi_\gamma \delta(\mathbf{k}_\alpha + \mathbf{k}_\beta + \mathbf{k}_\gamma) = \frac{2}{Q_{2D}} \delta(k_\alpha^z + k_\beta^z + k_\gamma^z), \quad (36)$$

where ϕ are the cylindrical angles and $Q_{2D} = \sqrt{4\rho_\beta^2\rho_\gamma^2 - (\rho_\beta^2 + \rho_\gamma^2 - \rho_\alpha^2)^2}$, is the area of the two-dimensional projection of the triangle formed by the resonant triad $\mathbf{k}_\alpha + \mathbf{k}_\beta + \mathbf{k}_\gamma = 0$. Here $\rho_\alpha = \sqrt{(k_\alpha^x)^2 + (k_\alpha^y)^2}$ denotes the projection of the absolute wave number k on the plane $k_z = 0$. The remaining integration of the collision integral is restricted to the domain $Q_{2D} \geq 0$. Details of the calculation is given in the appendix.

Because the spectrum is expected to be strongly concentrated near slow modes $k_\alpha^z = 0$, we approximate the averaged two-dimensional projected area of the resonant triangle by its three-dimensional counterpart. More precisely, we assume that the average of Q_{2D} with respect to the measure induced by the energy density is well approximated by the corresponding average of the three-dimensional triangle area,

$$\begin{aligned} \langle Q_{2D} \rangle &:= E^{-3} \int \int \int d\mathbf{k}_\alpha d\mathbf{k}_\beta d\mathbf{k}_\gamma Q_{2D} e_\alpha e_\beta e_\gamma \quad (37) \\ &\sim E^{-3} \int \int \int d\mathbf{k}_\alpha d\mathbf{k}_\beta d\mathbf{k}_\gamma Q_{3D} e_\alpha e_\beta e_\gamma = \langle Q_{3D} \rangle. \end{aligned}$$

with E being the total energy $E := \int d\mathbf{k}_\alpha e_\alpha$ and $Q_{3D} = \sqrt{4k_\beta^2 k_\gamma^2 - (k_\beta^2 + k_\gamma^2 - k_\alpha^2)^2}$. Under this approximation, the collision integral becomes

$$\begin{aligned} \partial_t e_\alpha &= \sum_{\beta, \gamma} \int_{\Theta(Q_{3D})} d \cos \theta_\beta d \cos \theta_\gamma k_\beta^2 dk_\beta k_\gamma^2 dk_\gamma k_\alpha^z \\ &\quad \frac{2\Gamma_{\alpha\beta\gamma}^2}{Q_{3D}} (k_\alpha^z e_\beta e_\gamma + k_\beta^z e_\alpha e_\gamma + k_\gamma^z e_\alpha e_\beta) \\ &\quad \delta(\omega_\alpha + \omega_\beta + \omega_\gamma) \delta(k_\alpha^z + k_\beta^z + k_\gamma^z), \quad (38) \end{aligned}$$

where $\Theta(Q_{3D})$ is the Heaviside function that limits the integration on the set of wavenumbers where the area of the triangle is non-negative.

Substituting the spectral ansatz introduced earlier (24), the kinetic equation is separable in the variables k and $\cos \theta$. The homogeneity degree of the angular part of the collision integral with respect to $\cos \theta_k$ is $-2f_w$; the contributions from the remaining terms cancel due to the homogeneity of the delta functions. Treating the angular spectrum as a generalized zero of the angular collision integral in the principal-value sense around $\theta_k = \pi/2$, yields $2f_w = -1$. This determines the angular part of the energy spectrum

$$e_\alpha = C_0 k^{-3} |\cos \theta_k|^{-1/2}. \quad (39)$$

For the helicity cascade on the positive branch the angular exponent remains the same, $f_{w,h} = f_{w_0}$, giving

$$e_\alpha^H = C_0 k^{-3.5} |\cos \theta_k|^{-1/2}. \quad (40)$$

Under the approximation described above, sign-definite helicity interactions therefore drive a portion of the energy flux toward large scales, consistent with the mechanism discussed in the previous section.

For comparison, [11], de Wit et al. derived the energy turbulent spectrum assuming the strongly anisotropic limit where k is replaced by its planar projection ρ through the kinetic equation. This renders the kinetic equation separable in ρ and k_z and leads to the scaling $e_\alpha \propto \rho^{-2.5} |k_z|^{-0.5}$. In spherical coordinates this

corresponds to $e_\alpha \propto k^{-3} |\cos \theta_k|^{-0.5} |\sin \theta_k|^{-2.5}$, which contains an unphysical divergence along $\theta = 0$.

The spectrum derived here avoids this pathology. Our result separates naturally into two parts: an isotropic scaling k^{-3} , which follows directly from the structure of the kinetic equation without additional assumptions, and an angular part $|\cos \theta_k|^{-1/2}$, obtained under the mild approximation introduced above. This yields a spectrum that remains regular away from the slow-mode curve while capturing the expected energy accumulation near $\theta = \pi/2$.

Implications to inertial waves. We now consider the case of inertial waves in a rapidly rotating fluid. Unlike the case of odd waves, the vector of frequencies $(\omega_\alpha, \omega_\beta, \omega_\gamma)$ on the resonant manifold is orthogonal both to $(1, 1, 1)$ and the helicity vector $(S_\alpha, S_\beta, S_\gamma)$. As a consequence, the interaction coefficients simplify to

$$(C_\alpha^{\beta\gamma}, C_\beta^{\alpha\gamma}, C_\gamma^{\alpha\beta}) = \Gamma_{\alpha\beta\gamma}(\omega_\alpha, \omega_\beta, \omega_\gamma), \quad (41)$$

And thus, in this case the kinetic equation takes the form

$$\partial_t e_\alpha = \sum_{\beta, \gamma} \int_{\omega_{\alpha\beta\gamma}} \omega_\alpha \Gamma_{\alpha\beta\gamma}^2 (\omega_\alpha e_\beta e_\gamma + \omega_\beta e_\alpha e_\gamma + \omega_\gamma e_\alpha e_\beta). \quad (42)$$

Despite this structural difference in the interaction coefficients, the turbulent spectrum obtained under the approximation introduced earlier (37) for the projected triangle area coincides with the one derived for odd waves,

$$e_\alpha = C_0 k^{-3} |\cos \theta_k|^{-1/2}. \quad (43)$$

The same weak singularity $|\cos \theta_k|^{-1/2}$ reflects the concentration of energy near the slow-mode manifold $k_z \approx 0$, consistent with the strongly anisotropic behavior predicted in the classical theory of inertial-wave turbulence in rotating fluids [7, 21, 22].

The same reasoning also applies to the helicity cascade on the positive branch. In particular, the helicity cascade solution and the conclusion that sign-definite helicity interactions drive a portion of the energy flux toward large scales remain valid for inertial waves as well.

Family of solutions in the very anisotropic limit and numerical evaluation of our findings

We now demonstrate numerically the results described above in the standard strongly anisotropic limit, where the magnitude of the wavenumber is approximated by its planar projection, $k \sim \rho$.

The normalized angular collision integral $\cos \theta_k S t_\Omega$, is homogeneous of degree zero in the angular variable $\cos \theta$. We verify numerically that the pair (w_0, f_{w_0}) corresponds to a zero of this collision integral.

In addition to the turbulent solution, the numerical evaluation reveals a one-dimensional family of approximate solutions of the form $e_\alpha = k^{-w} |\cos \theta_k|^{-f_w}$,

with parameters approximately in the range $w \in [2.8, 3.2]$ and $f_w \in [0.44, 0.57]$. The turbulent solution lies within this family at the point $(w_0, f_{w_0}) = (3, 0.5)$. The set of zeros of the collision integral in the (w, f) plane is presented in Figure 2.

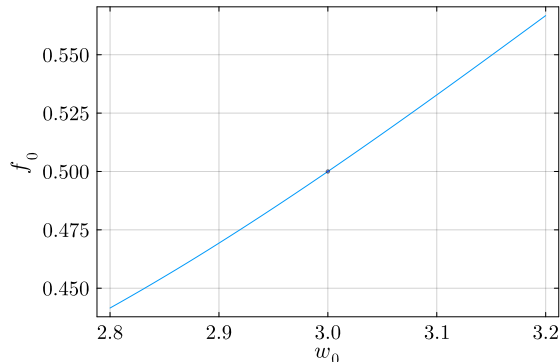


FIG. 2. Set of zeros of the collision integral, found numerically [23] in terms of the angular f_0 and radial w_0 power-laws. We highlight the energy cascade solution: $w_0 = 3$, $f_0 = 0.5$.

Next, we verify that sign-definite helicity interactions among waves belonging to the same helicity branch with $s_\alpha = s_\beta = s_\gamma$ transfer energy backwards in wave number k . That is, the contribution to the flux Π_α from interactions among the same branch is negative: $\Pi_\alpha|_{(+,+,+)} < 0$ for all ω_k . Normalized by the total flux, the contribution of triads $s_\alpha \neq s_\beta = s_\gamma$ is the smallest and the contribution of the triads $s_\alpha = s_\beta \neq s_\gamma$ and $s_\alpha = s_\gamma \neq s_\beta$ is positive to a forward cascade, so that $\Pi_\alpha|_{(+,-,+)} = \Pi_\alpha|_{(+,+, -)} > 0$. The total flux Π_α , and the fluxes restricted to the different triads $\Pi_\alpha|_{(+,+,+)}$, $\Pi_\alpha|_{(+,-,+)}$ and $\Pi_\alpha|_{(+,+, -)}$ are plotted in Figure 3.

These results reveal a clear separation between the roles of helicity-definite and helicity-mixed interactions. Triads composed of waves belonging to the same helicity branch drive energy toward larger spatial scales, while interactions involving waves of opposite helicity branches sustain the forward cascade. Consequently, although helicity is globally sign-indefinite, the decomposition into helicity branches introduces sign-definite interaction channels that systematically transfer a portion of the energy toward large scales.

This mechanism implies that when interactions between helicity branches are weakened—for example near a source emitting helicity-definite waves—the dynamics can favor an inverse transfer of energy. More generally, the results demonstrate that helicity organizes the cascade structure at the level of resonant triads, producing systematic backscatter even in regimes where the net energy cascade remains direct.

Conclusion and perspectives.

We studied weak turbulence in incompressible flows

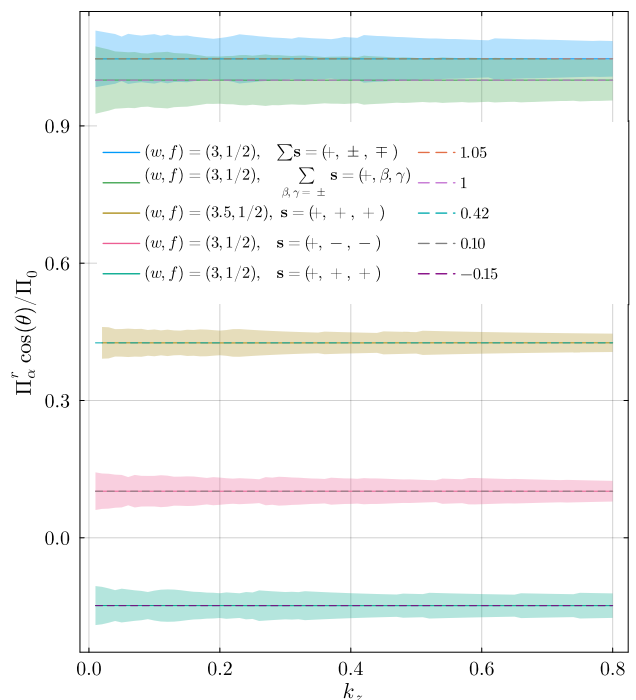


FIG. 3. Radial Fluxes of energy and helicity, as given by Eq. (32) (See appendix for the explicit form), as a function of k_α^z , evaluated at $k_\alpha = 1$. The fluxes were numerically integrated [24] and normalized to the total energy flux (blue line). Error regions correspond to ± 100 error estimation of the numerical integration.

with broken time-reversal symmetry. Our primary example is the case of odd-viscous (“odd”) waves, but all of our analytical arguments and conclusions extend directly to rotating Euler flow (inertial waves), with the corresponding substitutions in the dispersion relation and resonant geometry. In both systems the wave component admits a kinetic description whose collision integral inherits two quadratic invariants—energy and helicity—but reorganizes them in a strongly anisotropic manner. This setting provides a natural framework for understanding how a sign-indefinite invariant can nevertheless impose constraints on turbulent cascades.

Our first main result is a flux-based selection principle for the steady, scale-invariant spectrum. By introducing a natural gauge fixing for the energy flux, choosing a purely radial flux in \mathbf{k} space, we showed that among the dilation-invariant family $e_\alpha = C_0 k^{-w} e^\Omega(\theta_k)$ there is a unique exponent supporting a nonzero, divergence-free radial energy flux in the inertial range: $w = w_0 = 3$. This identifies the isotropic scaling of the turbulent state without invoking a strongly anisotropic reduction of the kinetic equation. The angular dependence is then determined by the geometry of the resonant manifold. Under a mild approximation motivated by the accumulation of energy near slow modes, we obtained the

asymptotic angular spectrum

$$e_\alpha = C_0 k^{-3} |\cos \theta_k|^{-1/2} = C_0 k^{-2.5} |\omega_k / \nu^{\text{odd}}|^{-0.5}, \quad (44)$$

which is singular only at $\omega_\alpha \rightarrow 0$ (the slow-mode curve) and avoids the nonphysical divergence at $\theta_k \rightarrow 0$ that appears when the strongly anisotropic limit is imposed too early.

Our second main result concerns the role of helicity in determining cascade directions. Although helicity is globally sign-indefinite in three dimensions, the helical decomposition splits it into sign-definite components on each polarization branch. We showed that triads whose three legs belong to the same helicity branch behave as if constrained by a sign-definite invariant and drive an upscale transfer of energy. In contrast, mixed-helicity triads support the usual downscale transfer. As a result, even in regimes where the total energy cascade is direct, helicity induces a systematic backscatter carried by sign-definite triads. In the limiting case where one branch dominates—for example under helicity-definite forcing—the kinetic equation admits an additional scaling associated with helicity transport, $e_\alpha \propto k^{-3.5} |\cos \theta_k|^{-1/2}$, and the energy transfer becomes predominantly inverse, mirroring the familiar role of sign-definite invariants in isotropic turbulence.

We substantiated these analytical conclusions by direct numerical evaluation of the collision integral in the standard strongly anisotropic limit. In that setting we observed (i) a one-parameter family of zeros of the normalized angular collision integral containing the turbulent solution $(w_0, f_0) = (3, 1/2)$, and (ii) a robust decomposition of the energy flux into helicity classes, with same-branch triads contributing a negative (upscale) flux and mixed-branch triads contributing a positive (downscale) flux.

Several directions follow naturally from this work. First, the slow-mode singularity highlights the limits of the diagonal, Gaussian closure underlying weak turbulence theory: arbitrarily small frequencies enter the collision integral as the system size grows, suggesting that a refined kinetic description incorporating near-resonant interactions and off-diagonal correlations may be required to fully describe the interface between waves and slow modes.

An alternative approach is to introduce a physical regularization that separates the wave manifold from the slow modes. One possible mechanism is the addition of weak stratification, which lifts the degeneracy at zero frequency. This is analogous to the treatment of internal inertia-gravity waves in strongly stratified flows, where a small rotation rate was introduced to regularize the kinetic equation and separate slow and wave dynamics [25].

A second direction is to investigate the Casimir structure associated with helicity in these systems. Understanding how helicity appears as a Casimir of

the underlying fluid dynamics may reveal additional constraints on the turbulent state beyond those captured by the kinetic equation, and could clarify how sign-indefinite invariants organize cascade directions in anisotropic wave turbulence.

Finally, although odd waves and inertial waves share the same turbulent spectrum within the framework developed here, their interaction structures and symmetry properties differ. A systematic comparison of the two systems may therefore reveal dynamical regimes where their cascade behavior diverges, shedding further light on the role of parity breaking and non-Hermitian wave dynamics in turbulence. This direction would naturally extend the comparison between rotating fluids and odd-viscous hydrodynamics initiated in [9] to the regime of wave turbulence.

Acknowledgments. We thank Jalal Shatah, Gregory Falkovich and Anna Frishman for many fruitful discussions. This work was supported by the Simons Foundation and the Simons Collaboration on Wave Turbulence. S. A. S. is supported by the CHE/PBC Fellowship.

APPENDIX

To evaluate $\delta E / \delta \omega$, note that

$$\delta E = \int \mathbf{v} \cdot \delta \mathbf{v} \, d\mathbf{x} = \int (\nabla \times \boldsymbol{\psi}) \cdot \delta \mathbf{v} \, d\mathbf{x} = \int \boldsymbol{\psi} \cdot \delta \boldsymbol{\omega} \, d\mathbf{x}, \quad (45)$$

where $\boldsymbol{\psi}$ is a divergence-free vector potential defined by $\nabla \times \boldsymbol{\psi} = \mathbf{v}$. Substituting into (2) recovers the Euler equation (1) exactly. The helicity H is a *Casimir* of the Poisson structure (3), it is conserved because the velocity \mathbf{v} lies in the kernel of \mathcal{J} . Indeed,

$$\begin{aligned} \partial_t H &= 2 \int \mathbf{v} \cdot \partial_t \boldsymbol{\omega} \, d\mathbf{x} = 2 \int \mathbf{v} \cdot \mathcal{J} \frac{\delta E}{\delta \boldsymbol{\omega}} \, d\mathbf{x} \\ &= -2 \int \mathcal{J} \mathbf{v} \cdot \frac{\delta E}{\delta \boldsymbol{\omega}} \, d\mathbf{x} = 0, \end{aligned} \quad (46)$$

where skew-symmetry of \mathcal{J} and $\mathcal{J} \mathbf{v} = 0$ imply the result.

PARAMETRIZATION OF THE RESONANT MANIFOLD

Consider the collision integral of a triad of waves forming a triangle, as given in Eq. (21), with the energy density given by Eq. (24). This homogeneous solution makes the collision integral separable, so the angular part decouples from the rest of the integration and can be solved separately, as shown below.

We work in cylindrical coordinates $\mathbf{k}_\alpha = (\rho_\alpha, \phi_\alpha, k_\alpha^z)$, and express the volume integration in terms of

$$\left(k_\alpha \equiv \sqrt{\rho_\alpha^2 + k_\alpha^z{}^2}, \phi_\alpha, k_\alpha^z \right):$$

$$\int dV_\alpha = \int \rho_\alpha d\rho_\alpha \int d\phi_\alpha \int dk_\alpha^z = \int k_\alpha dk_\alpha \int d\phi_\alpha \int dk_\alpha^z. \quad (47)$$

The collision integral then reads:

$$\begin{aligned} \partial_t e_k &= \sum_{\beta, \gamma} \iint k_\beta dk_\beta dk_\beta^z \iint k_\gamma dk_\gamma dk_\gamma^z k_\alpha^z |\Gamma_{\alpha\beta\gamma}|^2 \\ &\quad (k_\alpha^z e_\beta e_\gamma + k_\beta^z e_\alpha e_\gamma + k_\gamma^z e_\alpha e_\beta) \delta(\omega_\alpha + \omega_\beta + \omega_\gamma) \\ &\quad \delta(k_\alpha^z + k_\beta^z + k_\gamma^z) I_\phi, \end{aligned} \quad (48)$$

where we define

$$\begin{aligned} I_\phi &\equiv \iint d\phi_\beta d\phi_\gamma \delta(\rho_\alpha \cos(\phi_\alpha) + \rho_\beta \cos(\phi_\beta) + \rho_\gamma \cos(\phi_\gamma)) \\ &\quad \delta(\rho_\alpha \sin(\phi_\alpha) + \rho_\beta \sin(\phi_\beta) + \rho_\gamma \sin(\phi_\gamma)) \end{aligned} \quad (49)$$

As mentioned, the angular integral, I_ϕ , can be solved separately by the following change of variables:

$$s = \rho_\alpha \cos(\phi_\alpha) + \rho_\beta \cos(\phi_\beta) + \rho_\gamma \cos(\phi_\gamma), \quad (50)$$

$$t = \rho_\alpha \sin(\phi_\alpha) + \rho_\beta \sin(\phi_\beta) + \rho_\gamma \sin(\phi_\gamma). \quad (51)$$

Substituting back, with the Jacobian, the integral reads:

$$I_\phi = \iint \frac{1}{\rho_\beta \rho_\gamma \sin(\phi_\beta - \phi_\gamma)} \delta(s) \delta(t) ds dt. \quad (52)$$

To perform the integration, we rewrite the sine as a function of (s, t) and set them to zero:

$$\begin{aligned} \rho_\beta \rho_\gamma \sin(\phi_\beta - \phi_\gamma)|_{s=t=0} &= \pm \sqrt{\rho_\beta^2 \rho_\gamma^2 - \frac{1}{4} (\rho_\beta^2 + \rho_\gamma^2 - \rho_\alpha^2)^2} \\ &\equiv \pm \frac{Q_{2D}}{2}. \end{aligned} \quad (53)$$

We note that Q_{2D} corresponds to the area enclosed by the triangle of ρ_α , ρ_β and ρ_γ via Heron's formula. Alternatively, one can think of the area enclosed by the triangle of three vectors \mathbf{k}_α , \mathbf{k}_β and \mathbf{k}_γ , projected on the XY plane.

When we consider the geometrical interpretation of the above equation, it is clear that the negative branch does not participate: $\sin(\phi_\beta - \phi_\gamma)$ is the sine of an angle in a triangle; therefore, it must be positive. Finally:

$$I_\phi = \frac{2}{Q_{2D}}. \quad (54)$$

We return to Eqn. (48), and use the dispersion relation calculated in Eq. (12):

$$\delta(\omega_\alpha + \omega_\beta + \omega_\gamma) = \frac{\delta(\alpha k_\alpha^z k_\alpha + \beta k_\beta^z k_\beta + \gamma k_\gamma^z k_\gamma)}{|\nu_{\text{odd}}|}. \quad (55)$$

Lastly, the interaction term is given by [17]:

$$|\Gamma_{\alpha\beta\gamma}|^2 = \frac{Q_{3D}^2}{2^6 k_\alpha^z{}^2 k_\alpha^2 k_\beta^2 k_\gamma^2} (\beta k_\beta - \gamma k_\gamma)^2 (\alpha k_\alpha + \beta k_\beta + \gamma k_\gamma)^2, \quad (56)$$

$$Q_{3D} \equiv +\sqrt{4k_\beta^2 k_\gamma^2 - (k_\beta^2 + k_\gamma^2 - k_\alpha^2)^2}. \quad (57)$$

Using the bi-homogeneous spectrum (24) with $\cos(\theta) = \frac{k_\alpha^z}{k_\alpha}$, the sum over interaction coefficients reads

$$\begin{aligned} k_z e_\beta e_\gamma + p_z e_\alpha e_\gamma + q_z e_\alpha e_\beta &= C_0^2 \left(k_\alpha^z (k_\beta k_\gamma)^{-w+f} |k_\beta^z k_\gamma^z|^{-f} \right. \\ &\quad \left. + k_\beta^z (k_\alpha k_\gamma)^{-w+f} |k_\alpha^z k_\gamma^z|^{-f} + \dots \right. \\ &\quad \left. + k_\gamma^z (k_\alpha k_\beta)^{-w+f} |k_\alpha^z k_\beta^z|^{-f} \right). \end{aligned} \quad (58)$$

We can now substitute all of the above and perform the integration over k_γ^z using the delta function:

$$\begin{aligned} \partial_t e_k &= \sum_{\beta, \gamma} \int dk_\beta \int_{-k_\beta}^{k_\beta} dk_\gamma^z \frac{C_0^2 Q_{3D}^2}{2^5 Q_{2D} k_\alpha^z k_\alpha^2 k_\beta k_\gamma} \\ &\quad (\beta k_\beta - \gamma k_\gamma)^2 (\alpha k_\alpha + \beta k_\beta + \gamma k_\gamma)^2 \times \dots \\ &\quad \frac{\delta(\alpha k_\alpha^z k_\alpha + \beta k_\beta^z k_\beta - \gamma(k_\alpha^z + k_\beta^z) k_\gamma)}{|\nu_{\text{odd}}|} \\ &\quad \left(k_\alpha^z (k_\beta k_\gamma)^{-w+f} |k_\beta^z (k_\alpha^z + k_\beta^z)|^{-f} + \right. \\ &\quad \left. k_\beta^z (k_\alpha k_\gamma)^{-w+f} |k_\alpha^z (k_\alpha^z + k_\beta^z)|^{-f} - \right. \\ &\quad \left. (k_\alpha^z + k_\beta^z) (k_\alpha k_\beta)^{-w+f} |k_\alpha^z k_\beta^z|^{-f} \right). \end{aligned} \quad (59)$$

We note that, in general, since k_γ^z is bounded by k_γ via $|k_\gamma^z| \leq k_\gamma$, we must ensure k_β^z obeys:

$$\begin{aligned} |k_\alpha^z + k_\beta^z| &\leq k_\gamma \\ \max\{-k_\beta, -k_\gamma - k_\alpha^z\} &\leq k_\beta^z \leq \min\{k_\beta, k_\gamma - k_\alpha^z\}. \end{aligned} \quad (60)$$

EVALUATING THE COLLISION INTEGRAL, IN THE VERY ANISOTROPIC APPROXIMATION

Proceeding, we assume the very **anisotropic limit** where the projection of each wave-vector on the z -direction is much smaller than the absolute value of the wave: $k_\alpha \gg k_\alpha^z, k_\beta \gg k_\beta^z, k_\gamma \gg k_\gamma^z$. As a result, the condition described in Eq. (60) is trivially satisfied. Moreover, the 2D area is approximated by the 3D area, further simplifying the calculation.

Using properties of the delta function:

$$\delta(\alpha k_\alpha^z k_\alpha + \beta k_\beta^z k_\beta - \gamma(k_\alpha^z + k_\beta^z) k_\gamma) = \frac{\delta(k_\beta^z - k_\alpha^z \frac{\gamma k_\gamma - \alpha k_\alpha}{\beta k_\beta - \gamma k_\gamma})}{|\beta k_\beta - \gamma k_\gamma|}. \quad (61)$$

In the special case where $k_\beta = k_\gamma$ and $\beta = \gamma$, the delta function is proportional to $\delta(k_\alpha^z (\alpha k_\alpha - \beta k_\beta))$ requiring that either k_α^z vanishes (see discussion on slow modes in the main text), or an equilateral triangle in 3D $k_\alpha = k_\beta = k_\gamma$, on the branch: $\alpha = \beta = \gamma$.

Thus, the collision integral reads:

$$\begin{aligned} \partial_t e_k = & \sum_{\beta, \gamma} \int dk_\beta \int dk_\gamma \frac{C_0^2 Q_{3D}}{2^5 |\nu_{\text{odd}}| k_\alpha^2 k_\alpha^2 k_\beta k_\gamma} \\ & |\beta k_\beta - \gamma k_\gamma| (\alpha k_\alpha + \beta k_\beta + \gamma k_\gamma)^2 \left(k_\alpha^z (k_\beta k_\gamma) \right)^{-w+f} \\ & \left| (k_\alpha^z)^2 \frac{\gamma k_\gamma - \alpha k_\alpha}{\beta k_\beta - \gamma k_\gamma} \frac{\beta k_\beta - \alpha k_\alpha}{\beta k_\beta - \gamma k_\gamma} \right|^{-f} + \\ & k_\alpha^z \frac{\gamma k_\gamma - \alpha k_\alpha}{\beta k_\beta - \gamma k_\gamma} (k_\alpha k_\gamma)^{-w+f} \left| (k_\alpha^z)^2 \frac{\beta k_\beta - \alpha k_\alpha}{\beta k_\beta - \gamma k_\gamma} \right|^{-f} \\ & - k_\alpha^z \frac{\beta k_\beta - \alpha k_\alpha}{\beta k_\beta - \gamma k_\gamma} (k_\alpha k_\beta)^{-w+f} \left| (k_\alpha^z)^2 \frac{\gamma k_\gamma - \alpha k_\alpha}{\beta k_\beta - \gamma k_\gamma} \right|^{-f} \Bigg). \end{aligned} \quad (62)$$

It is now apparent that around the singular point of an equilateral triangle, namely when the difference between each pair of k 's scales like $\tilde{\epsilon}$ and $\alpha = \beta = \gamma$, the integrand scales like $\tilde{\epsilon}$ and its limit should vanish. However, this introduces numerical instability, which we shall later address.

Additionally, it is important to note that the integration limits on the set of k 's must obey the triangle inequality. Following [26, 27], we will compute the integration limits within the kinematic box. Moreover, it is convenient to perform the following change of variables to (u, v) :

$$k_\alpha < k_\beta + k_\gamma \longrightarrow u \equiv \frac{k_\beta + k_\gamma}{2k_\alpha} > \frac{1}{2}, \quad (63)$$

$$k_\beta < k_\alpha + k_\gamma \longrightarrow v \equiv \frac{k_\beta - k_\gamma}{2k_\alpha} < \frac{1}{2}, \quad (64)$$

$$k_\gamma < k_\alpha + k_\beta \longrightarrow v \equiv \frac{k_\beta - k_\gamma}{2k_\alpha} > -\frac{1}{2}, \quad (65)$$

Accordingly, the integral transforms as:

$$\int dk_\beta \int dk_\gamma = 2k_\alpha^2 \int_{\frac{1}{2}}^{\infty} du \int_{-\frac{1}{2}}^{\frac{1}{2}} dv. \quad (66)$$

In the new parameters (u, v) , the kinetic equation in the

very anisotropic limit reads:

$$\begin{aligned} \partial_t e_k = & \sum_{\beta, \gamma} \int_{\frac{1}{2}}^{\infty} du \int_{-\frac{1}{2}}^{\frac{1}{2}} dv \frac{C_0^2 \sqrt{(4u^2 - 1)(1 - 4v^2)}}{2^4 |\nu_{\text{odd}}| (u^2 - v^2)} \\ & |u(\beta - \gamma) + v(\beta + \gamma)| (\alpha + u(\beta + \gamma) + v(\beta - \gamma))^2 \\ & k_\alpha^{3-2w+2f} |k_\alpha^z|^{-2f} \left((u^2 - v^2)^{-w+f} \right. \\ & \left. \left| \frac{(\alpha - \beta(u + v)) (\alpha - \gamma(u - v))}{(u(\beta - \gamma) + v(\beta + \gamma))^2} \right|^{-f} - \right. \\ & \left. \frac{\alpha - \gamma(u - v)}{u(\beta - \gamma) + v(\beta + \gamma)} (u - v)^{-w+f} \right. \\ & \left. \left| \frac{\alpha - \beta(u + v)}{u(\beta - \gamma) + v(\beta + \gamma)} \right|^{-f} + \frac{\alpha - \beta(u + v)}{u(\beta - \gamma) + v(\beta + \gamma)} \right. \\ & \left. (u + v)^{-w+f} \left| \frac{\alpha - \gamma(u - v)}{u(\beta - \gamma) + v(\beta + \gamma)} \right|^{-f} \right). \end{aligned} \quad (67)$$

Accordingly, the radial flux is given, using Eq. (32), by

$$\begin{aligned} \Pi_\alpha^r(w_0) = & \frac{C_0^2}{2k_\alpha^{d-1}} \frac{d}{dw} St_\Omega \Big|_{w=w_0} \quad (68) \\ = & \frac{1}{2k_\alpha^{d-1}} \frac{d}{dw} \left(\frac{1}{k_\alpha^{d-2w}} St_\alpha \right) \Big|_{w=w_0} \\ = & - (k_\alpha)^{2f-(d-1)} |k_\alpha^z|^{-2f} \sum_{\beta, \gamma} \int_{\frac{1}{2}}^{\infty} du \int_{-\frac{1}{2}}^{\frac{1}{2}} dv \\ & \frac{C_0^2 \sqrt{(4u^2 - 1)(1 - 4v^2)}}{2^5 |\nu_{\text{odd}}| (u^2 - v^2)} |u(\beta - \gamma) + v(\beta + \gamma)| \\ & (\alpha + u(\beta + \gamma) + v(\beta - \gamma))^2 \left((u^2 - v^2)^{-w_0+f} \right. \\ & \ln(u^2 - v^2) \left| \frac{(\alpha - \beta(u + v)) (\alpha - \gamma(u - v))}{(u(\beta - \gamma) + v(\beta + \gamma))^2} \right|^{-f} - \\ & \frac{\alpha - \gamma(u - v)}{u(\beta - \gamma) + v(\beta + \gamma)} (u - v)^{-w_0+f} \ln(u - v) \\ & \left. \left| \frac{\alpha - \beta(u + v)}{u(\beta - \gamma) + v(\beta + \gamma)} \right|^{-f} + \frac{\alpha - \beta(u + v)}{u(\beta - \gamma) + v(\beta + \gamma)} \right. \\ & \left. (u + v)^{-w_0+f} \ln(u + v) \left| \frac{\alpha - \gamma(u - v)}{u(\beta - \gamma) + v(\beta + \gamma)} \right|^{-f} \right). \end{aligned} \quad (69)$$

NUMERICAL EVALUATION

The collision integral given in Eq. (67) can be easily evaluated using HCubature module in the Julia programming language [24]: a multidimensional integration computed adaptively, by dividing the integration volume into smaller sections, until it

converges.

To avoid numerical instabilities, we emphasize an exclusion of three areas: First, $u \approx \frac{1}{2}$, and $v \approx (\pm \frac{1}{2})$, which correspond to zero area, that is, they bear zero weight, and are therefore safely excluded. Moreover, assuming f is positive, NaN results are obtained for the following cases:

- For $u - v = 1$, $\gamma = \alpha$,
- For $v = 0$, $\beta = \gamma$,
- For $u + v = 1$, $\beta = \alpha$.

All of these result from an equilateral triangle, as can be seen from the delta function (61). Although these points introduce a numerical instability, their analytical limit vanishes, as explained below Eq. (62).

Numerically, we introduce two regulators, h and d , such that:

- We replace $v \in (\frac{1}{2}, \infty)$ by $u \in [\frac{1}{2} + 10^{-d}, 10^h]$.
- We replace $u \in (-\frac{1}{2}, \frac{1}{2})$ by
 - When $\beta \neq \gamma$: $v \in [-\frac{1}{2} + 10^{-d}, \frac{1}{2} - 10^{-d}]$
 - When $\beta = \gamma$: $v \in [-\frac{1}{2} + 10^{-d}, -10^{-d}]$ & $[10^{-d}, \frac{1}{2} - 10^{-d}]$.

The original limits are recovered at the limit $(h, d) \rightarrow \infty$, however, both the kinetic equation and fluxes saturate as a function of said regulators. The values of the regulators, h and d , were chosen to allow both convergence to the physical value and convergence of the numerical evaluation.

To find the steady states of $e_k(w, f)$, we used the ‘find_zero’ function from the ‘Roots’ package in Julia [23].

-
- [1] A. N. Kolmogorov, The local structure of turbulence in incompressible viscous fluid for very large reynolds numbers, *Proceedings of the Royal Society of London. Series A: Mathematical and Physical Sciences* **434**, 9 (1991).
- [2] R. H. Kraichnan, *Inertial ranges in two-dimensional turbulence*, Tech. Rep. (1967).
- [3] R. Fjørtoft, On the changes in the spectral distribution of kinetic energy for two-dimensional, nondivergent flow, *Tellus* **5**, 225 (1953).
- [4] V. E. Zakharov, V. S. L’vov, and G. Falkovich, *Kolmogorov Spectra of Turbulence I: Wave Turbulence* (Springer, 1992).
- [5] H. Poincaré, Sur l’équilibre d’une masse fluide animée d’un mouvement de rotation, *Bulletin astronomique, Observatoire de Paris* **2**, 109 (1885).
- [6] H. P. Greenspan, *The theory of rotating fluids*. (Cambridge University Press, 1969).
- [7] S. Galtier, Weak inertial-wave turbulence theory, *Physical Review E* **68**, 015301 (2003).
- [8] J. Avron, Odd viscosity, *Journal of statistical physics* **92**, 543 (1998).
- [9] X. M. de Wit, M. Fruchart, T. Khain, F. Toschi, and V. Vitelli, Pattern formation by turbulent cascades, *Nature* **627**, 515 (2024).
- [10] M. Fruchart, C. Scheibner, and V. Vitelli, Odd viscosity and odd elasticity, *Annual Review of Condensed Matter Physics* **14**, 471 (2023).
- [11] X. M. de Wit, S. Galtier, M. Fruchart, F. Toschi, and V. Vitelli, Non-hermitian wave turbulence, arXiv preprint arXiv:2504.15403 (2025).
- [12] S. Chen, X. M. De Wit, M. Fruchart, F. Toschi, and V. Vitelli, Odd viscosity suppresses intermittency in direct turbulent cascades, *Physical Review Letters* **133**, 144002 (2024).
- [13] S. Gomé and A. Frishman, Helicity controls the direction of fluxes in rotating turbulence, arXiv preprint arXiv:2512.05253 (2025).
- [14] S. Gomé and A. Frishman, Waves drive the rise and fall of 2d flows in rotating turbulence, arXiv preprint arXiv:2509.18323 (2025).
- [15] P. J. Olver, A nonlinear hamiltonian structure for the euler equations, *Journal of Mathematical Analysis and Applications* **89**, 233 (1982).
- [16] Supplemental material, including additional derivation and technical information.
- [17] F. Waleffe, The nature of triad interactions in homogeneous turbulence, *Physics of Fluids A: Fluid Dynamics* **4**, 350 (1992).
- [18] M. Shavit, O. Bühler, and J. Shatah, Sign-indefinite invariants shape turbulent cascades, *Physical Review Letters* **133**, 014001 (2024).
- [19] V. E. Zakharov, V. S. L’vov, and G. Falkovich, *Kolmogorov spectra of turbulence I: Wave turbulence* (Springer Science & Business Media, 2012).
- [20] S. Nazarenko, *Wave turbulence*, Vol. 825 (Springer Science & Business Media, 2011).
- [21] C. Cambon, N. N. Mansour, and F. S. Godeferd, Energy transfer in rotating turbulence, *Journal of Fluid Mechanics* **337**, 303 (1997).
- [22] C. Cambon, R. Rubinstein, and F. S. Godeferd, Advances in wave turbulence: rapidly rotating flows, *New Journal of Physics* **6**, 73 (2004).
- [23] J. Verzani, Roots.jl: Root finding functions for julia, <https://github.com/JuliaMath/Roots.jl> (2020).
- [24] S. G. Johnson, The HCubature.jl package for multi-dimensional adaptive integration in Julia, <https://github.com/JuliaMath/HCubature.jl> (2017).
- [25] M. Shavit, O. Bühler, and J. Shatah, Wave turbulence of inertia-gravity waves: a theory for the oceanic spectrum, arXiv preprint arXiv:2601.01476 (2026).
- [26] V. Labarre, N. Lanchon, P.-P. Cortet, G. Krstulovic, and S. Nazarenko, On the kinetics of internal gravity waves beyond the hydrostatic regime, *Journal of Fluid Mechanics* **998**, A17 (2024).
- [27] Y. V. Lvov, K. L. Polzin, and N. Yokoyama, Resonant and near-resonant internal wave interactions, *Journal of Physical Oceanography* **42**, 669 (2012).